ELSEVIER

Nuclear Instruments and Methods in Physics Research B 193 (2002) 172–177

NIM B
Beam Interactions with Materials & Atoms

www.elsevier.com/locate/nimb

Channeling energy loss of O ions in Si: The Barkas effect

L.L. Araujo [a], P.L. Grande [a,*], M. Behar [a], J.F. Dias [a], J.H.R. dos Santos [a], G. Schiwietz [b]

[a] *Instituto de Física – Universidade Federal do Rio Grande do Sul Caixa Postal 15051, Av. Bento Gonçalvez 9500, CEP 91501 – 970, Porto Alegre (RS), Brazil*

[b] *Hahn-Meitner-Institüt, Bereich Festkörperphysick Glienicker Strasse 100, 14109 Berlin, Germany*

Abstract

In this work we report on measurements of channeling stopping powers of ^{16}O ions along Si⟨1 0 0⟩ axial direction for the energy range between 250 keV/u and 1 MeV/u by using the Rutherford backscattering technique with separated by implanted oxygen targets. In connection with the recent developed unitary convolution approximation, we are able to extract the Barkas contribution to the energy loss with high precision. This effect is clearly separated from other processes and amounts to about 15%. The observed Barkas contribution from the valence-electron gas is in agreement with the Lindhard model for higher energies. However, in contrast to recent investigations for Li ions, the Barkas effect at the lowest energies seems to saturate, indicating other non-perturbative terms in the polarization field induced by the O ions in Si.

1. Introduction

The stopping force of light and heavy projectiles under channeling conditions has been investigated during the last years in order to improve the fundamental understanding of ion–solid interactions. Important issues related to the energy loss in the polarization field are still unclear [1,2]. Only recently [1], the so-called Barkas effect, an energy-loss enhancement proportional to the third power of the projectile charge at high energies, has been clearly separated from other processes, and reaches huge relative values for Li ions channeling along the Si⟨1 1 0⟩ direction.

There is a general lack of information concerning the slowing down from medium to heavy ions in crystals. These data are also important for ion beam analysis and modification of materials. A large amount of data related to H impinging along the Si major directions is available. Conversely, despite the fact that He beams are often used in Rutherford backscattering (RBS)/channeling analysis of Si samples, only recently the stopping data have been reported for the Si⟨1 0 0⟩ channel [3–5]. Concerning heavier ions, channeling stopping data are scarce and generally restricted to narrow energy ranges [6–11].

Here, we report on measurements of the electronic stopping power as a function of the incidence energy for oxygen channeling along Si⟨1 0 0⟩ direction. For these measurements, we have used the RBS channeling technique in combination with a separated by implanted oxygen (SIMOX) target.

* Corresponding author.
E-mail address: grande@if.ufrgs.br (P.L. Grande).

0168-583X/02/$ - see front matter
PII: S0168-583X(02)00745-0

The advantage of the present experimental arrangement lies in the fact that it circumvents the use of thin self-supported films, which are required in transmission measurements. In addition, the present technique allows stopping power measurements down to low energies. Consequently, we were able to measure in a relatively wide energy range, between 4 and 15 MeV.

Special emphasis will be devoted to the determination of Barkas effect of O ions under channeling conditions. According to previous results for He and Li projectiles [1,12], such a channeling investigation has many advantages, compared to measurements performed in amorphous targets or at a random direction. Firstly, disturbing effects such as shell corrections, electron capture, or other inner-shell effects that overshadow the Barkas term are strongly reduced. Secondly, channeling conditions provide the best scenario for the applicability of electron-gas models. The Barkas contribution is then obtained as in [1] by subtracting theoretical results from the experimental data. The results of these calculations take into account the ion-flux distribution and the impact-parameter dependent energy loss for each projectile charge-state, according to the unitary convolution approximation (UCA) [13].

2. Experimental procedure and data analysis

We have used SIMOX type samples consisting of 2000 Å Si$\langle 100 \rangle$ crystal layers on top of 4000 Å SiO_2 buried layers, produced in $\langle 100 \rangle$ Si wafers. The samples were prepared at IBM (T.J. Watson Research Center, New York). For each experiment, the sample was cleaned and etched to remove the native oxide film on the surface using a 10% HF acid right before the RBS measurements.

The energy-loss measurements were carried out using the ion beam (with energy E_0) impinging on the sample at channeling and random directions. The backscattered ^{16}O particles were detected by a Si surface-barrier heavy ion detector (EG&G, A27, 6 keV noise width) located at 170° with respect to the incident beam. The overall resolution of the detection system was about 30 keV for O. Typical RBS spectra taken at random and channeling directions for O ions at an incident energy of $E_0 = 13$ MeV are shown in Fig. 1. In this figure, E_c and E_r are the detected energies of the backscattered particles at the Si/SiO_2 interface for the channeled and random incidences, respectively. These energies were determined by fitting the channeling and random spectra with an algorithm [14], which includes, in addition to the error function (accounting for particle straggling and detector resolution), the energy dependence of the Rutherford cross-section. Finally, in the framework of the mean energy approximation, it can be shown [3] that the channeling specific energy loss along the projectile incoming path (before the backscattering) is a function of the energies E_0, E_c and E_r, the specific energy loss in a random direction, and geometrical factors. We have used the random energy loss data from [15]. Details of the data evaluation can be found elsewhere [14].

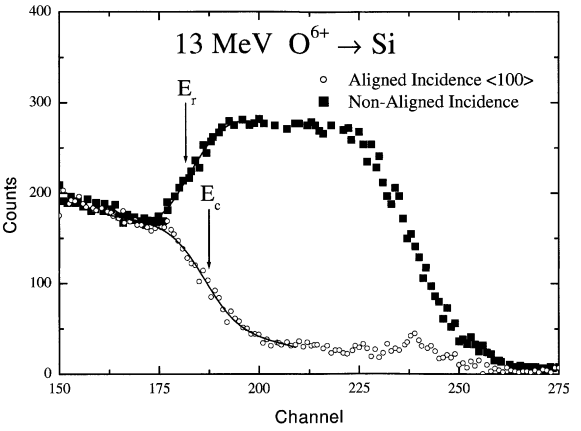

Fig. 1. RBS spectra for 13 MeV O^{6+}+Si for random and channeled directions. In this figure, E_c and E_r stand for the detected energies of the backscattered particles at the Si/SiO_2 interface for channeling and random conditions respectively. Full lines represent the results of the fitting procedure [14] used to determine the corresponding energy loss.

At this point, it is important to stress that the channeling stopping power depends on the target thickness because of the ion flux distribution and the projectile charge-state. For very thin crystals, the ion flux distribution is nearly uniform and the projectile charge-state is equal to the incident one. Then, assuming that the effect of the pre-equilibrium projectile charge-state is of minor importance

(because an incident charge-state close to the equilibrium value can be chosen), the channeling stopping power will be nearly identical to the random one. After less than 2000 Å, equilibrated ion flux distributions [3] and projectile charge-states [16] are achieved. On the other hand, if the crystal is too thick, the channeling stopping power may also approach the random one, due to dechanneling at crystal defects, thermal vibrations and electronic multiple scattering. The SIMOX target (2000 Å) used in this experiment is thick enough to prevent pre-equilibrium ion flux distribution and thin enough to avoid enhanced dechanneling effects.

3. Theoretical procedure

Under axial channeling conditions, the energy loss due to the Si inner-shell electrons is strongly suppressed, since the ion flux distribution along a major axial direction has a peak in the middle of the channel (flux peaking). Hence, the mean energy lost by the projectile after passing a certain thickness X is given by the general formula

$$\Delta E = \frac{\int_A \mathrm{d}^2\rho \int_0^X \mathrm{d}x \frac{\mathrm{d}E(\vec{\rho})}{\mathrm{d}x} \Phi(\vec{\rho},x)}{\int_A \mathrm{d}^2\rho \int_0^X \mathrm{d}x \Phi(\vec{\rho},x)}, \tag{1}$$

where A is the transversal area of the Si axial channel, $\vec{\rho}$ the position relative to the center of the channel, $\Phi(\vec{\rho},x)$ the ion flux distribution at the distance $\vec{\rho}$ and depth x (along the channeling direction). The energy loss per traversed distance $\frac{\mathrm{d}E}{\mathrm{d}x}(\vec{\rho})$ may be divided into two contributions,

$$\frac{\mathrm{d}E}{\mathrm{d}x}(\vec{\rho}) = \left(\frac{\mathrm{d}E}{\mathrm{d}x}(\vec{\rho})\right)_{\text{direct}} + \left(\frac{\mathrm{d}E}{\mathrm{d}x}(\vec{\rho})\right)_{\text{e-loss}}. \tag{2}$$

The first contribution corresponds to the energy loss involving the Si electrons (target ionization/excitation and electron capture), while the second one is due to energy loss from electrons originally bound to the projectile (projectile ionization/excitation). Both contributions can be obtained from the impact parameter dependent energy loss $Q(b)$ in a binary collision between the projectile in a charge-state q with a neutral Si atom, as (for instance)

$$\left(\frac{\mathrm{d}E}{\mathrm{d}x}(\vec{\rho})\right)_{\text{direct}} = \sum_q f_q \sum_i \frac{Q^{(q)}_{\text{direct}}(b_i)}{d}, \tag{3}$$

where d is the interatomic distance along the Si⟨100⟩ axis and the index i labels all neighboring Si atoms. Since the projectiles may be found in different charge-states q, with fractions given by f_q, the average over the projectile charge-state has to be performed. The O charge-state distributions were taken from experiments performed under channeling conditions [11]. The ion flux distribution were obtained by calculating the O ion trajectories in a Monte Carlo simulation code [17].

The valence electron density sampled by the ions (no transverse space selection has been performed) using either Si atomic or 3D solid-state values from [18] deviates from each other by only 2.5%. Solid-state effects due to the Si valence electrons, namely the partially compensating collective screening and plasmon excitation, have implicitly been accounted for by normalizing the mean energy transfers of all shells to yield the Bethe value as extracted from experimental solid-state data. Within first-order perturbation theory, the results of our method (without Bloch terms) agree with full band-structure calculations for protons in Si [18] to about 3% for the total stopping power as well as for the channeling energy loss.

The energy loss $Q(b)$ in a single collision at an impact parameter b plays a very important role in the determination of the stopping power under channeling conditions. In fact, the reduction of the stopping power for channeled ions is due to a significant suppression of collisions with small impact parameters. Here, we adopt the Unitary Convolution Approximation (UCA) as described in [12,13]. In this method, the energy loss in different impact-parameter regions is well determined and interpolated smoothly. The physical inputs of the model are the projectile-screening function (in the case of dressed ions), the electron density and oscillators strengths of the target atoms. Moreover, the convolution approximation, in the perturbative mode (called PCA), yields remarkable agreement with full semi-classical-approximation (SCA) results for bare as well as for screened ions for all impact parameters. In the unitary mode

(called UCA), the method contains some higher-order effects (providing in some cases fairly good agreement with full coupled-channel calculations) and approaches the classical regime through the Bohr model for large perturbations ($Z/v \gg 1$).

4. Results and discussion

According to the procedure outlined in Section 2, we have determined the energy loss of ^{16}O ions along the Si$\langle 1\,0\,0\rangle$ direction. The results are presented in Fig. 2 together with the channeling data by Jiang et al. [11]. The quoted errors have been estimated from the statistical dispersion of the measurements. An inspection of Fig. 2 indicates that the ratio of channeling to random stopping powers is about 80% at the lowest energy and decreases down to 60% at 15 MeV. This behavior reflects the role of the valence and inner-shell electrons. Indeed, for increasing projectile energies, the contribution of the inner-shell electrons to the random stopping power increases, whereas the contribution from these electrons are almost completely suppressed under axial channeling conditions.

A comparison of our results (closed symbols) with previous experimental channeling data (open symbols) [11], obtained by using the transmission technique, is also depicted in Fig. 2. As can be observed, there is a general good agreement between the two experimental data. In fact, the overall difference is less than 5% and is within the experimental errors. It should be stressed that the previous channeling data have been measured using thick targets (about 10 000 Å). This fact may introduce a slight overestimation of the channeling energy-loss due to dechanneling at crystal defects and electronic multiple scattering. These effects are expected to be more important for impinging light ions (Li ions [12]) than for heavier projectiles such as O.

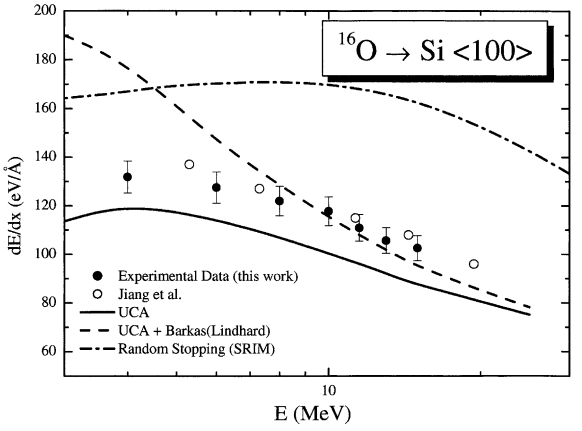

Fig. 2. Energy loss of O ions as a function of the ion energy for the $\langle 1\,0\,0\rangle$ direction of Si. Full circles: this work; solid line: UCA model; open circles: Jiang et al. [11]; dash-dotted line: random stopping power by Ziegler et al. (SRIM) [22]; dashed line UCA calculation with Barkas correction after Lindhard [19].

As shown in Fig. 2, the UCA calculations underestimate the channeling experimental data for all studied energies. It has been shown [1] that this difference comes from polarization effects, which are not included in the present calculations. Indeed, the UCA calculations do not contain any higher-order effect proportional to an odd power of the projectile charge. Therefore, the Barkas contribution to the channeling energy loss can be taken as the difference between the experimental data and the UCA calculations. The effect is about 10–15% and is nearly energy independent for the present energy range.

Fig. 2 also shows the UCA calculations with the Barkas contribution added according to the Lindhard model [19]. The Lindhard formula accounts for the polarization effect due to the Si valence electrons, and reads (in atomic units)

$$\left(\frac{\mathrm{d}E}{\mathrm{d}x}\right)_{\mathrm{Barkas}} = \left(\frac{Z_1\omega_\mathrm{p}}{v}\right)^3 \frac{3\pi}{2v^2} \ln\left(\frac{2v^2}{\omega_\mathrm{p}}\right), \qquad (4)$$

where ω_p is the plasmon energy. This correction, as in [1], was implemented by using the average projectile charge-state to the third power $\langle q^3\rangle$ and by considering the four valence electrons of Si (with $\omega_\mathrm{p} = 16.6$ eV) to be homogeneously distributed in the solid. The latter assumption implies that the Barkas correction is the same for random and channeling directions. This assumption is well justified [20] for the Si$\langle 1\,0\,0\rangle$ direction, because the electron density is nearly uniform across the channel. Contrary to the case of He and Li, the Lindhard's model describes well the experimental

data only for energies $E > 600$ keV/u. At lower energies, the Lindhard model, which is based on perturbation theory, is not valid anymore. That means that other terms proportional to Z^5, Z^7, and so on gain importance for decreasing energy and other non-perturbative approaches [21] must be used.

The absolute value of the Barkas contribution increases with increasing projectile atomic number. This behavior is shown in Fig. 3 for He, Li (from [1]) and O channeling along Si⟨100⟩ at four different velocities. The dotted line corresponds to a contribution proportional to the third power of the charge-state (the Lindhard contribution). In fact, since in this energy range the ions have many non-negligible charge-states, we have plotted all curves as a function of the mean charge-state. The dotted curve agrees very well with the data at the highest projectile velocity, but at lower energies strong deviations are observed. In fact a tendency to saturation is noted. The solid curves are obtained by interpolation of the present oxygen data together with previous ones for Li and He. At 500 keV/u, the slope of the curve is influenced by a contribution proportional to the fifth power of the mean charge-state (q^5). However, at lower energies other terms proportional to (q^{2n+1}, $n > 2$) are important. It is worth pointing out that the solid curves should be regarded with some caution, because there are only three data points for the fit.

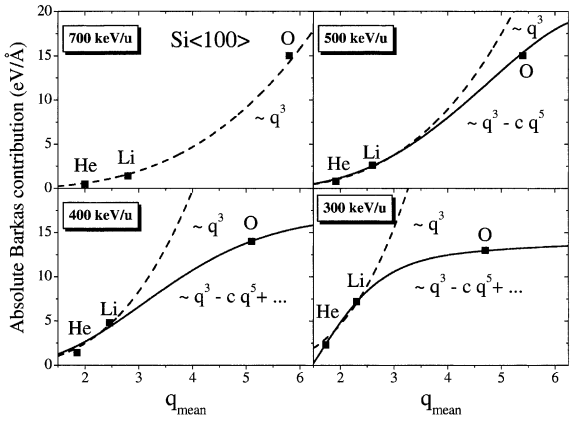

Fig. 3. Absolute Barkas effect (experimental channeling data subtracted from UCA calculations) as a function of the mean charge-state for He and Li from [1] and O (this work). Dotted lines correspond to a contribution proportional to the mean projectile charge to the third power. Solid lines represent a monotonous interpolation function (containing only q to odd powers).

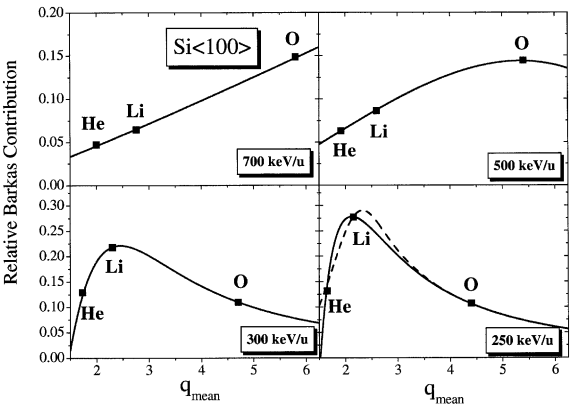

Fig. 4. Relative Barkas effect as a function of the mean charge-state for He and Li from [1] and O (this work). Solid lines correspond to a monotonous interpolation function (containing only q to odd powers). The dashed line at 250 keV/u represents another choice of interpolation function.

The relative Barkas effect under channeling conditions is a little more complicated function, since the total channeling stopping power and the Barkas contribution increase with the atomic number at different rates. The ratio between the experimentally determined Barkas effect and the UCA calculations is presented in Fig. 4 for four different ion velocities. At 700 keV/u, we observe a monotonous dependence of the relative Barkas contribution on the mean charge-state, from less than 5% for He up to 15% for O ions. For decreasing ion velocities, a maximum is found around Li. The maximum value of the Barkas contribution is about 30% at 250 keV/u and it is even higher (about 50%) for Li at 150–200 keV/u [1]. The dashed line shows another interpolation method indicating the error in the determination of the maximum.

5. Conclusions

In the present work, we have measured the channeling stopping power of ^{16}O along the Si⟨100⟩ direction. For the channeling measurements we have used the RBS technique associated

with a SIMOX target. This method allows for measurements in a wide energy range without using self-supported crystals.

We have also determined the contribution of the Barkas effect for the Si valence electrons with channeled O projectiles. The combination of the channeling RBS method and the recent theoretical realization of the impact-parameter dependence of the Bethe–Bloch contribution (the UCA calculations) has allowed for a clear quantitative determination of the Barkas effect. The maximum polarization enhancement of the stopping power is about 15%. Contrary to which was observed for Li and He, the Barkas effect for O projectiles is nearly energy independent and has a strong saturation at lower projectiles velocities. It was also shown that the maximum relative Barkas effect may be found for Li or Be projectiles. This maximum is determined by the saturation of the Barkas contribution found for heavier projectiles.

The channeling energy loss provides the best scenario to test theoretical predictions, and the present oxygen results call for refined models of non-perturbative polarization effects.

Acknowledgements

This work was partially supported by the Brazilian agencies Conselho Nacional de Desenvolvimento Científico e Tecnológico (CNPq) and CAPES-DAAD (Brazilian–German) international cooperation program (PROBRAL).

References

[1] G. De M. Azevedo, P.L. Grande, M. Behar, J.F. Dias, G. Schiwietz, Phys. Rev. Lett. 86 (2001) 1482.
[2] P. Sigmund, A. Schinner, Phys. Rev. Lett. 86 (2001) 1486.
[3] J.H.R. dos Santos, P.L. Grande, M. Behar, H. Boudinov, G. Schiwietz, Phys. Rev. B 55 (1997) 4332.
[4] G. Lulli, E. Albertazzi, M. Bianconi, G.G. Bentini, R. Nipoti, R. Lotti, Nucl. Instr. and Meth. B 170 (2000) 1.
[5] Y. Yamamoto, A. Ikeda, T. Yoneda, K. Kajiyama, Y. Kido, Nucl. Instr. and Meth. B 153 (1999) 10.
[6] S. Datz, J. Gomes de Campo, P.P. Dittner, P.D. Miller, J.A. Biggerstaff, Phys. Rev. Lett. 38 (1977) 1145.
[7] J.A. Golovchenko, A.N. Goland, J.S. Rosner, C.E. Thorn, H.E. Wegner, H. Knudsen, C.D. Moak, Phys. Rev. B 23 (1981) 957;
J.A. Golovchenko, D.E. Cox, A.N. Goland, Phys. Rev. B 26 (1982) 2335.
[8] J.H.R. dos Santos, M. Behar, P.L. Grande, H. Boudinov, Phys. Rev. B 55 (1997) 13651.
[9] D. Niemann, G. Konac, S. Kalbitzer, Nucl. Instr. and Meth. B 118 (1996) 11.
[10] G.G. Bentini, M. Bianconi, R. Nipoti, F. Malaguti, E. Verondini, Nucl. Instr. and Meth. B 53 (1991) 1.
[11] W. Jiang, R. Grötzschel, W. Pilz, B. Schmidt, W. Möller, Phys. Rev. B 59 (1999) 226;
W. Jiang, R. Grötzschel, W. Pilz, B. Schmidt, W. Möller, Phys. Rev. B 60 (1999) 714.
[12] G. De M. Azevedo, P.L. Grande, M. Behar, J.F. Dias, D.L. da Silva, G. Schiwietz, submitted for publication.
[13] G. Schiwietz, P.L. Grande, Nucl. Instr. and Meth. B 153 (1999) 1;
P.L. Grande, G. Schiwietz, Phys. Rev. A 58 (1998) 3796, http://www.hmi.de/people/schiwietz/casp.html.
[14] J.H.R. dos Santos, P.L. Grande, H. Boudinov, M. Behar, R. Stoll, Chr. Klatt, S. Kalbitzer, Nucl Instr. and Meth. B 106 (1994) 51.
[15] L.L. Araujo, M. Behar, J.F. Bias, P.L. Grande, J.H.R. dos Santos, Nucl. Instr. and Meth. B 190 (2002) 79.
[16] G De, M. Azevedo, J.R.A. Kaschny, J.F. Dias, P.L. Grande, M. Behar, Ch. Klatt, S. Kalbitzer, Nucl. Instr. and Meth. B 148 (1999) 168.
[17] J.H. Barret, Phys. Rev. B 3 (1971) 1527.
[18] J.M. Pitarke, I. Campillo, Nucl. Instr. and Meth. B 164–165 (2000) 147.
[19] J. Lindhard, Nucl. Instr. and Meth. 132 (1976) 1.
[20] P.L. Grande, G. Schiwietz, Nucl. Instr. and Meth. B 136–138 (1998) 125.
[21] P. Sigmund, A. Schinner, Eur. Phys. J. D 12 (2000) 425.
[22] SRIM program from J.F. Ziegler homepage;
J.F. Ziegler, J.P. Biersack, U. Littmark, The Stopping and Range of Ions in Solids, Pergamon, New York, 1985.